ACS Catalysis

Research Article

pubs.acs.org/acscatalysis

High-Pressure XPS of Crotyl Alcohol Selective Oxidation over Metallic and Oxidized Pd(111)

Adam F. Lee,*[,†] James N. Naughton,[‡] Zhi Liu,[§] and Karen Wilson*[,†]

[†]Cardiff Catalysis Institute, School of Chemistry, Cardiff University, Cardiff, CF10 3AT, U.K.

[‡]Department of Chemistry, University of York, Heslington, York, YO10 5DD, U.K.

[§]Advanced Light Source, Lawrence Berkeley Laboratory, 1 Cyclotron Road, Berkeley, California 94720, United States

Supporting Information

ABSTRACT: Here, we report on the first application of high-pressure XPS (HP-XPS) to the surface catalyzed selective oxidation of a hydrocarbon over palladium, wherein the reactivity of metal and oxide surfaces in directing the oxidative dehydrogenation of crotyl alcohol (CrOH) to crotonaldehyde (CrHCO) is evaluated. Crotonaldehyde formation is disfavored over Pd(111) under all reaction conditions, with only crotyl alcohol decomposition observed. In contrast, 2D Pd_5O_4 and 3D PdO overlayers are able to selectively oxidize crotyl alcohol (1 mTorr) to crotonaldehyde in the presence of co-fed oxygen (140 mTorr) at temperatures as low as 40 °C. However, 2D Pd_5O_4 ultrathin films are unstable toward reduction by the alcohol at ambient temperature, whereas the 3D PdO oxide is able to sustain catalytic crotonaldehyde production even up to 150 °C. Co-fed oxygen is essential to stabilize palladium surface oxides toward in situ reduction by crotyl alcohol, with stability increasing with oxide film dimensionality.

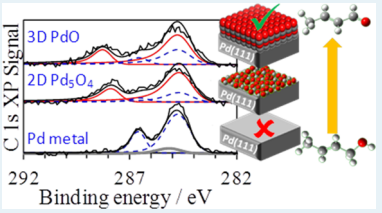

KEYWORDS: *selective oxidation, palladium, high-pressure XPS, alcohol, in situ*

INTRODUCTION

Aerobic selective oxidation of alcohols (selox) represents an elegant class of atom-efficient molecular transformations that yield valuable aldehyde, ketone acid, and ester products that find application across the fine chemical, pharmaceutical, and agrochemical sectors. Commercial selox processes have traditionally employed stoichiometric oxidants or homogeneous metal catalysts (or both); however, the quest for sustainable chemistry is now driving the search for alternative solid catalyst technologies that offer lower hazardous and toxic waste, simple product separation, and continuous processing in fixed-bed reactors.[1] Allylic aldehydes are high-value components used in the perfume and flavorings industries[2] and can be readily synthesized under mild conditions by the oxidative dehydrogenation of their corresponding alcohol over platinum-group and noble metal heterogeneous catalysts:[3] Crotonaldehyde is an important agrochemical and valuable precursor to the food preservative sorbic acid, and citronellyl acetate confers rose/fruity flavors and aroma.

The direct, aerobic selective oxidation of functionalized hydrocarbons via platinum-group metal catalysts has been a matter of intense research and debate over the past decade.[4,5] Early ex situ mechanistic studies exploring alcohol selox by platinum-group metals suggested that reduced (metallic) species were responsible for effecting the catalytic cycle; however, these were compromised by the use of corrosive electrolytes[6] or strongly adsorbing surfactants. There is now compelling evidence from operando XAS measurements[7] and structure−activity studies over well-defined catalysts[8−10] that in the case of palladium, oxide and not metal is, in fact, the active catalytic species. In vacuo temperature-programmed XPS and mass spectrometry investigations of crotyl alcohol (but-2-en-1-ol) and crotonaldehyde (but-2-en-1-al) over Au/Pd(111)[11,12] surfaces have demonstrated that oxidative dehydrogenation of the alcohol competes with decarbonylation of the aldehyde over palladium metal (Scheme 1)[13,14] and that coadsorbed oxygen or alloyed gold can ameliorate the latter pathway.[14,15] Definitive proof that the outermost layers of palladium are oxidized during selox under realistic conditions has remained

Scheme 1. CrOH Oxidation to CrHCO Showing Undesired Competing Decarbonylation Pathway

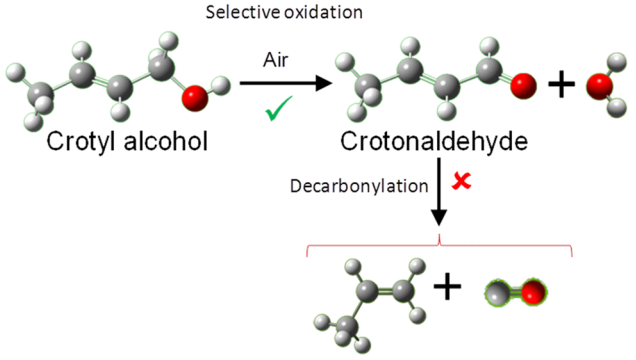

Special Issue: Operando and In Situ Studies of Catalysis

Received: July 6, 2012
Revised: August 15, 2012
Published: September 17, 2012

   dx.doi.org/10.1021/cs300450y | ACS Catal. 2012, 2, 2235−2241

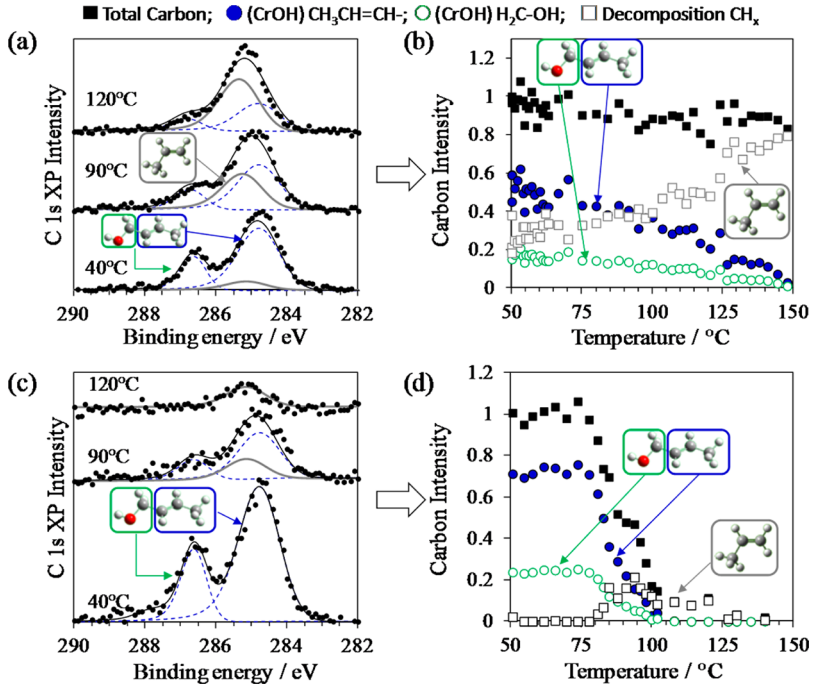

Figure 1. Surface chemistry of CrOH over Pd(111). Snapshot C 1s XP spectra for CrOH adlayer adsorbed at 40 °C over Pd(111) and heated to 150 °C either (a) in vacuo or (c) under 140 mTorr O_2 while continuously acquiring spectra. Intensities of fitted C 1s components from the entire series of spectra during the temperature-programmed reaction are shown in parts b and d. Note a single envelope is used to simplify fitting of the C_3 component of CrOH and alkylidyne decomposition species.

elusive though, because of the inherent instability of palladium surface oxides in the preceding (in vacuo) model studies and lack of surface sensitivity in the operando techniques brought to bear on dispersed Pd nanoparticles to date.

Pioneering work in analyzer and vacuum prelens chamber design in the 1970s[16,17] has paved the way for the development of HP-XPS or ambient pressure photoelectron spectroscopy, (AP-PES)[18−24] which can bridge the "pressure gap", thereby permitting the study of metastable phases,[22,25] and identification of adsorbates present during steady state catalytic turnover.[26−29] HP-XPS has recently been employed to study the oxidation of palladium single crystals at pressures up to 1 Torr,[30−32] enabling the construction of detailed phase diagrams spanning several distinct surface and bulk oxide phases which map well to theoretical predictions. Herein, we utilize this knowledge to investigate the surface chemistry of crotyl alcohol by HP-XPS over two-dimensional Pd_5O_4 and three-dimensional PdO surface oxides prepared on a Pd(111) substrate and compare their reactivity with that of the underlying metal as a function of oxygen partial pressure and temperature.

■ EXPERIMENTAL SECTION

HP-XPS measurements were conducted on BL 9.3.2 of the Advanced Light Source (ALS), Lawrence Berkeley National Laboratory,[20] operating at a beam energy and current of 1.9 GeV and 500 mA, respectively. The end station consists of a sample preparation chamber with a sputter gun and an analytical chamber equipped with a quadrupole mass spectrometer. The sample was mounted via tantalum clips to a ceramic button heater, and type K thermocouple wires were spot-welded to the edge of the Pd(111) crystal to measure sample temperature. Sample cleaning was performed by repeated sputter, 700 °C anneal, and O_2 treatment cycles, with final sample cleanliness verified by removal of surface carbon by XPS. The binding energy was calibrated with respect to the Fermi edge of the sample. Spectra were processed with CasaXPS Version 2.3.5, employing a Shirley background subtraction and spectral fitting using the lineshapes detailed in Supporting Information Table S1. Asymmetric Doniach Sunjic functions were used to fit both Pd 3d and C 1s regions, and symmetrical Gaussian−Lorentzian functions were used for the overlapping Pd $3p_{3/2}$ and O 1s regions. The choice of an asymmetric line shape for our high resolution C 1s XP spectra follows previous studies of adsorbed hydrocarbons on metal surfaces, wherein vibronic broadening induces asymmetry.[33] Spectra were fitted with the minimum number of peaks required to minimize the *R* factor, using components in a fixed intensity ratio of 3:1 for the $CH_3CH{=}CH-$ and $-COH/-C{=}O$ environments of crotyl alcohol/crotonaldehyde, respectively. Extra peaks were added as required to account for expected hydrocarbon fragments and C═O arising from molecular decomposition. The fwhm and binding energies of all peaks were held constant during fitting. Gas-phase ionization effects at pressures in the mTorr range eliminated charging of the thin oxide films.

Surface and bulk oxides were prepared following literature methods[31] by oxidation of Pd(111) either at 500 K under 140 mTorr O_2 (Pd_5O_4) or at 700 K under 500 mTorr O_2 (PdO) for 15 min, followed by cooling to 40 °C under O_2. The O 1s/Pd $3p_{3/2}$ region was measured at 835 eV photon energy, and C 1s and Pd 3d XP spectra were recorded at 595 and 650 eV photon energies, respectively. Crotyl alcohol (Fluka 95%, 1:19 cis/trans) was purified by repeated freeze−pump−thaw cycles prior to background vapor dosing at either 1×10^{-7} Torr or 1 mTorr through unheated stainless steel lines and valves to avoid thermal decomposition. Oxygen was co-fed at 140 mTorr.

dx.doi.org/10.1021/cs300450y | ACS Catal. 2012, 2, 2235−2241

RESULTS AND DISCUSSION

CrOH adsorption over Pd(111) was first examined to understand the chemistry of the clean metal and compare with our previous in vacuo study.[14] Figure 1a shows two well-resolved components in the C 1s spectra at 285 and 286.7 eV along with a weak component at 285.5 eV following a 200 Langmuir (L) CrOH exposure (at pressure of 5×10^{-7} Torr for 400 s) at 40 °C. The components at 285 and 286.7 eV are in a 3:1 ratio, which is consistent with the CH_3CHCH- and $-H_2C-OH$ functionalities of the parent CrOH, as reported following 150 K adsorption over Pd(111).[14] Molecular adsorption of the alcohol at this temperature is somewhat surprising, since our previous low temperature study suggests that a heated CrOH adlayer should undergo significant dehydrogenation and decarbonylation. We tentatively attribute this observation to the formation of a stabilized alkoxide ($CH_3CH{=}CHCH_2O-$) adlayer as a result of rapid decomposition and carbon lay-down of a small fraction of the initially adsorbing CrOH, with subsequent lateral interactions driving adoption of a tilted alkoxide with a smaller adsorption footprint, preventing further reaction. Surface carbon has previously been observed to stabilize ethanol as an alkoxide over Pt(111) at 295 K,[34] suppressing the usual complete decomposition seen following 150 K adsorption and heating.[35] This hypothesis is supported by a 0.3 eV chemical shift to lower binding energy apparent when comparing the RC−OH carbon in the present study with that reported following 150 K adsorption.[14] Indeed, the third C 1s component present at 285.5 eV grows upon heating the saturated adlayer and is indicative of an alkylidyne fragment. This state increases continuously with temperature (Figure 1b) at the expense of the alcohol/alkoxide to dominate the surface above 100 °C.[14,36] In the absence of coadsorbed oxygen, Pd(111) thus rapidly self-cokes at catalytically relevant temperatures (60−140 °C). Recent operando DRIFTS/MS/XAS measurements of reduced Pd nanoparticles have likewise reported the decomposition of CrOH above 120 °C, with concomitant transient evolution of reactively formed propene and CO preceding coking.[37]

The impact of gas-phase O_2 (at 140 mTorr) on the thermal chemistry of a saturated CrOH adlayer (200 L at 40 °C) was subsequently investigated, and the resulting C 1s XP spectra and fitted components are shown in Figure 1c−d. In contrast to the in vacuo heating, the presence of coadsorbed oxygen substantially suppresses decomposition pathways, with adsorbed CrOH (alkoxide) remaining intact at ≤75 °C, above which the vast majority of the alcohol desorbs, coincident with decomposition of ∼20% of the initial adlayer, both processes being complete by 100 °C. Higher temperatures promote combustion and removal of this residual surface carbon. A similar phenomenon was observed during the temperature-programmed reaction of propene in the presence of coadsorbed oxygen on Pd(111) under UHV conditions, wherein desorption of the intact alkene is promoted over dehydrogenation to propylidyne that characterizes the clean metal.[12] The mechanism by which background oxygen deactivates metallic palladium toward CrOH decomposition, for example, electronic through-substrate charge transfer or steric adsorbate−adsorbate repulsion, is the subject of ongoing quantum chemical modeling. Experiments in which CrOH (1 mTorr) was codosed with oxygen (140 mTorr) (Supporting Information Figure S1) likewise resulted only in the formation of a surface alkoxide species, with observed surface chemistry similar to that in Figure 1c upon heating under an oxygen background. This suggests alcohol decomposition pathways are extremely sensitive to the net redox environment, with metallic surfaces unable to selectively oxidize the alcohol through to the aldehyde, even under co-fed background oxygen, which is consistent with liquid phase selox studies over Pd/Al_2O_3 and Pd/SiO_2 wherein solvent oxygen depletion drives in situ reduction of PdO to Pd and concomitant rapid on-stream deactivation.[38]

Having demonstrated that Pd(111) was inactive toward the oxidative dehydrogenation of CrOH under any accessible conditions, the reactivity of palladium oxide surfaces was assessed. Successful generation of Pd_5O_4 and PdO surface oxides was verified by comparison with the spectral fingerprints provided in the work of Ketteler et al.[31] and Zemlynov et al.[32] Figure 2a, b shows the fitted O1s/Pd3p$_{3/2}$ and Pd 3d$_{5/2}$ XP

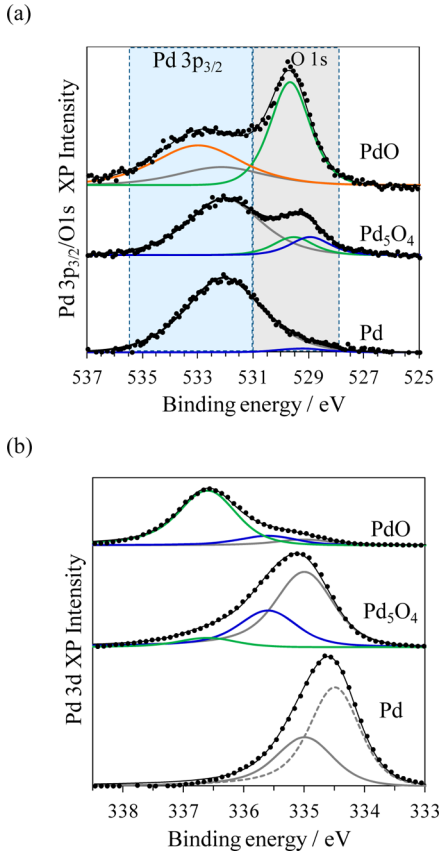

Figure 2. Fitted (a) Pd 3p$_{3/2}$ and O 1s XP spectra and (b) Pd 3d$_{5/2}$ XP spectra of clean Pd(111) and as-prepared Pd_5O_4/Pd(111) and PdO/Pd(111) surfaces.

spectra of clean Pd(111) and the associated 2D and 3D surface oxides. Although the Pd 3d$_{5/2}$ peak can be successfully fitted with bulk and surface core level components at 335 and 334.5 eV, respectively, as expected for clean Pd(111),[39] the corresponding Pd 3p$_{3/2}$/O1s region suggests a trace $O_{(a)}$ component is also present at 529 eV, in addition to the Pd 3p$_{3/2}$ feature at 532.3 eV. Following oxidation at 500 K under 140 mTorr O_2 to generate the two-dimensional surface oxide, Pd_5O_4, characteristic states at 529 and 529.7 eV originating from 3- and 4-fold coordinated O^{2-} sites appear (note: these were not resolvable in our measurements but are included in the fit for consistency with the literature). The corresponding

dx.doi.org/10.1021/cs300450y | ACS Catal. 2012, 2, 2235−2241

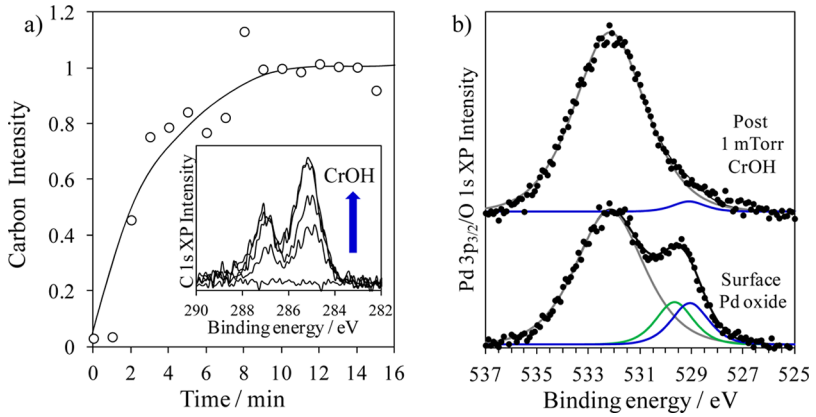

Figure 3. (a) Integrated C 1s XP total signal during exposure of Pd_5O_4/Pd(111) surface oxide to 1 mTorr CrOH at 40 °C and (b) O 1s spectra of Pd_5O_4/Pd(111) surfaces before and after CrOH adsorption.

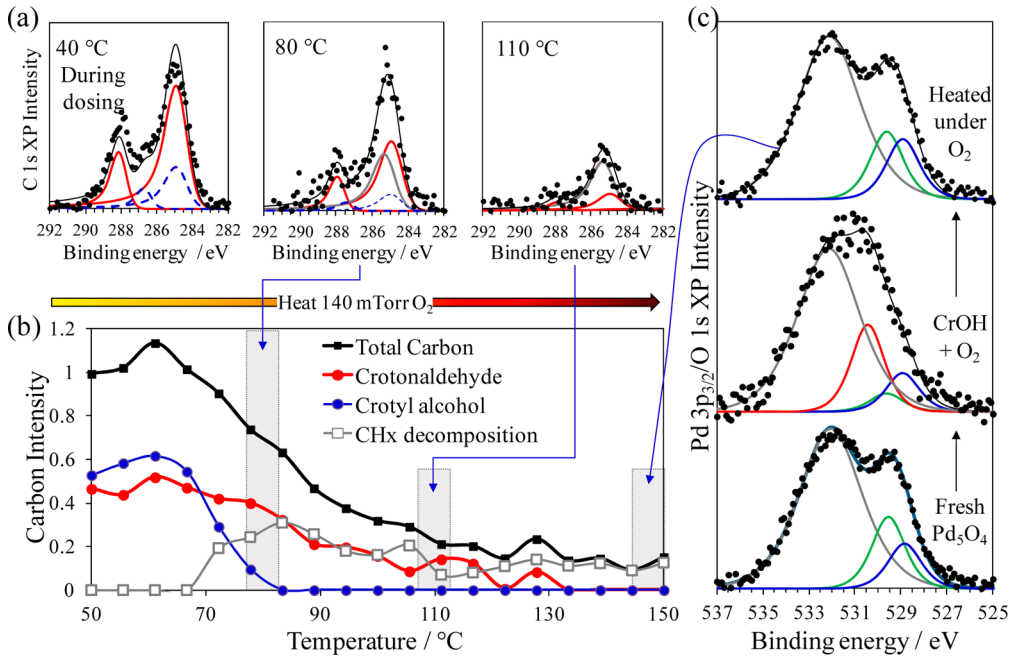

Figure 4. Surface chemistry of CrOH adsorption over Pd_5O_4/Pd(111): (a) snapshots of fitted C 1s XP spectra under 1 mTorr CrOH and 140 mTorr O_2 at 40 °C, subsequently heated to 80 and 110 °C under 140 mTorr O_2; (b) integrated C 1s XP total signal and fitted CrOH, CrHCO, and CH_X components during temperature-programmed reaction under oxygen; (c) corresponding O 1s XP spectra of as-prepared Pd_5O_4/Pd(111) surface and following exposure to CrOH/mixture at 40 °C and temperature-programmed reaction under O_2 to 150 °C.

Pd $3d_{5/2}$ spectra contained components at 335, 335.5, and 336.5 eV, attributed to Pd^0 and oxide phases in which Pd atoms are coordinated to two and four O^{2-} neighbors, respectively,[30] which is consistent with Pd_5O_4 formation. The retention of the 335 eV bulk Pd signal is a reflection of the 2D nature of this Pd_5O_4 surface, that is, the underlying metallic Pd features are not fully attenuated. Bulk PdO forms when a critical near-surface oxygen concentration is reached,[40] which was achieved following oxidation at 700 K under 500 mTorr O_2. Such treatment resulted in the growth of an intense O 1s peak at 529.7 eV and the evolution of Pd $3p_{3/2}$ and Pd $3d_{5/2}$ states at 533 and 336.5 eV states, respectively. The 3D nature of these PdO overlayers also results in strong attenuation of the metallic Pd components in the $3p_{3/2}$ and $3d_{5/2}$ spectra.

High-pressure CrOH adsorption (1 mTorr) was initially followed over the Pd_5O_4 surface oxide in the absence of background O_2, and the resulting C 1s spectra and integrated carbon coverage are presented in Figure 3a. As observed over Pd(111), CrOH adsorbs molecularly at 40 °C (or at least into the same indistinguishable alkoxide species), with monolayer saturation achieved after 10 min of dosing. However, inspection of the corresponding O 1s reveals that CrOH adsorption is accompanied by simultaneous reduction of the surface oxide (Figure 3b). Since no oxidized hydrocarbon adsorbates are detected during this process, we infer that oxygen abstracted from the Pd_5O_4 capping layer is lost from the surface as evolved water[37] through reaction with surface hydrogen arising during CrOH adsorption as an alkoxide.

In an attempt to stabilize the Pd_5O_4 surface oxide toward in situ reduction by CrOH, the same experiment was repeated while codosing 140 mTorr oxygen (Figure 4). Remarkably, after 16 min of codosing at 40 °C, a new chemical state appears in the C 1s XP spectra in Figure 4a at 288.2 eV, that is, at 1.2 eV higher binding energy that the −H**C**−OH component of the parent alcohol, characteristic of the −CH═O state expected upon crotonaldehyde formation.[14] Quantification of

dx.doi.org/10.1021/cs300450y | *ACS Catal.* 2012, 2, 2235−2241

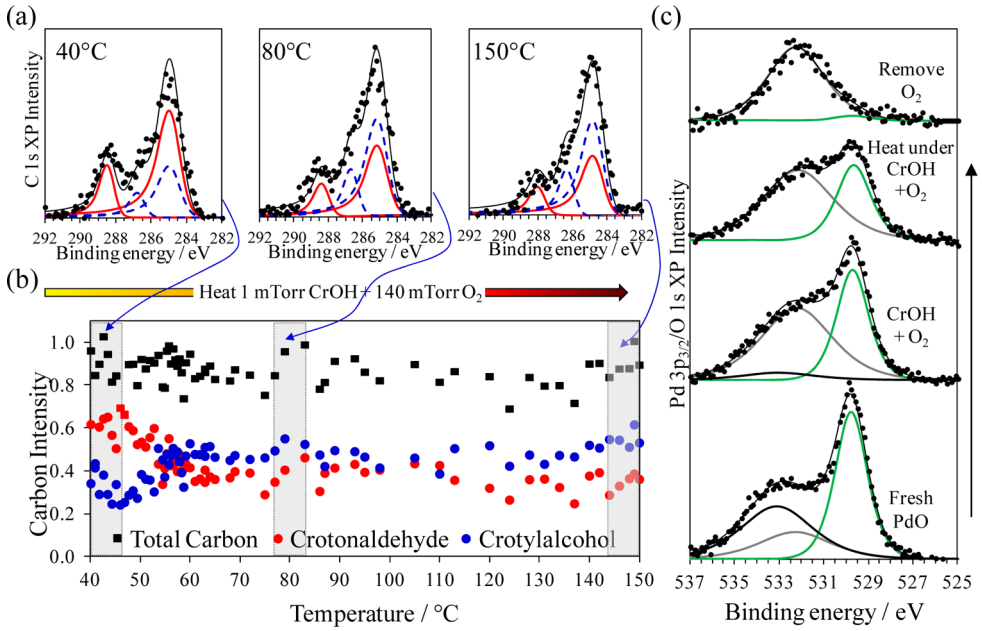

Figure 5. Surface chemistry of CrOH adsorption over PdO/Pd(111). (a) Snapshots of fitted C 1s XP spectra under 1 mTorr CrOH and 140 mTorr O_2 at 40 °C, subsequently heated to 80 and 150 °C under 1 mTorr CrOH and 140 mTorr O_2; (b) integrated C 1s XP total signal and fitted CrOH, CrHCO, and CH_X components during temperature-programmed reaction under CrOH and oxygen; (c) corresponding O 1s XP spectra of as-prepared PdO/Pd(111) surface and following exposure to CrOH/O_2 mixture at 40 °C, temperature-programmed reaction under CrOH/O_2 to 150 °C and, finally, removal of O_2 at 150 °C.

the integrated CH═O and associated CH_3CH═CH− components (Figure 4a) reveals ∼75% of the hydrocarbon adlayer exists as aldehyde during codosing. The corresponding O 1s XP spectra (Figure 4c) show that although in situ reduction of the surface oxide still occurs under CrOH + O_2 cofeeding, ∼30% of the original surface oxygen is retained. Reaction induces a redistribution of the surface oxygen species with a new state at 530.6 eV required to fit the O 1s spectra, which has previously been attributed to a metastable high-coverage chemisorbed oxygen species.[30]

The CrOH feedstream was subsequently removed, and the adsorbed adlayer was heated while maintaining the O_2 background pressure (Figure 4b). This resulted in the steady desorption of reactively formed crotonaldehyde and unreacted CrOH above 75 °C, accompanied by the growth of a state at 285.5 eV analogous to that observed over Pd(111) and attributed to alkylidyne formation. Over the oxide, only ∼15% of the initially adsorbed (decomposed) hydrocarbons remain on the surface by 150 °C, with surface cleanup through alcohol/aldehyde desorption coinciding with reoxidation of the palladium surface, as evidenced by the O 1s XP spectra in Figure 4c, again highlighting the critical interplay between the stability of palladium surface oxides and competitive adsorption of hydrocarbons versus oxygen as a function of their respective partial pressures, which is consistent with a Mars−van Krevelen process.[41,42] Reoxidation of supported palladium nanoparticles occurs rapidly at similar temperatures (albeit at higher oxygen partial pressures) upon switching from an oxygen-lean to -rich feedstream during vapor phase CrOH oxidation.[37] This represents the first direct evidence that a surface oxide of palladium is responsible for crotonaldehyde formation from crotyl alcohol; however, it is clear that the 2D Pd_5O_4 oxide layer is susceptible to reduction by adsorbed hydrocarbons and cannot thus sustain catalytic turnover under more reducing environments.

In light of the preceding instability of the Pd_5O_4 oxide toward in situ reduction, we examined the surface chemistry of the thicker 3D PdO film (Figure 5), for which attenuation of the underlying Pd metal 3d XP signal (to 20% of the clean surface value) suggests an oxide thickness of 0.9 nm, assuming an inelastic mean free path of 0.81 nm for 321 eV photoelectrons.[43]

Co-feeding the PdO/Pd(111) sample with CrOH (1 mTorr) and oxygen (140 mTorr) at 40 °C resulted in C 1s XP spectra similar to those seen over the Pd_5O_4 surface under the same conditions, with Figure 5a, b highlighting similar levels of CrHCO formation (∼67% of the entire adlayer). However, in contrast to the surface oxide, the corresponding O 1s XP spectra demonstrate that around 80% of the parent PdO remains, even after 1 h of continuous exposure to this CrOH/O_2 feed, with 60% retained following subsequent heating to 150 °C (Figure 5c). *Preservation of PdO now confers steady state crotonaldehyde production from a CrOH/O_2* reaction *mixture* at the highest temperatures investigated, with the surface comprising a 60:40 CrOH/CrHCO adlayer between 80 and 150 °C. Finally, the importance of maintaining a high oxygen partial pressure and, thus, fully oxidized palladium surface was verified by removing oxygen from the gas stream while continuing to dose 1 mTorr CrOH at 150 °C. Three minutes after oxygen removal, the O 1s XP spectra show complete loss of the PdO phase (Figure 5c), coincident with rapid accumulation of alkylidyne moieties at 285.8 eV (not shown), akin to those observed in Figure 1a at 120 °C.

In conclusion, HP-XPS has enabled us to conduct the first direct measurements of hydrocarbon oxidation over catalytically relevant model palladium surfaces and to compare the reactivity of Pd metal and oxides toward allylic alcohol selox (Figure 6 and Scheme 2). Pd(111) cannot catalyze the oxidative dehydrogenation of crotyl alcohol to crotonaldehyde under either pure alcohol or mixed alcohol/O_2 reactant

dx.doi.org/10.1021/cs300450y | *ACS Catal.* 2012, 2, 2235−2241

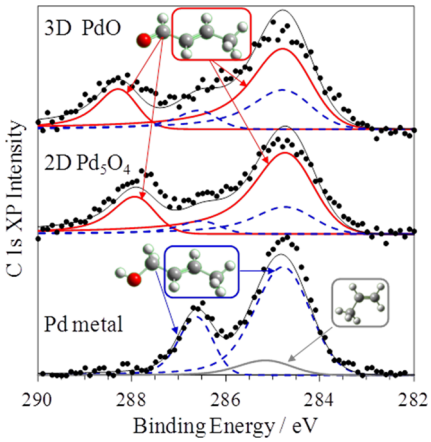

Figure 6. Summary of C 1s spectra for reaction products formed during 40 °C exposure of Pd to CrOH, and Pd_5O_4/Pd(111) and PdO/Pd(111) surfaces to CrOH under 140 mTorr O_2.

Scheme 2. CrOH Oxidation over Pd(111), Pd_5O_4/Pd(111), and PdO/Pd(111)[a]

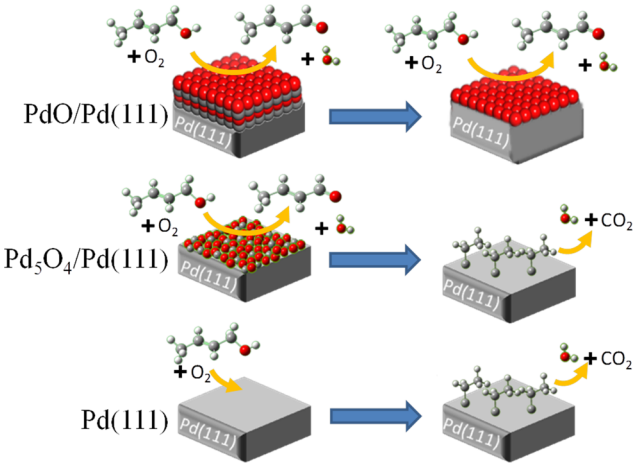

[a]Reaction over palladium metal leads to CrOH decomposition, whereas Pd_5O_4/Pd(111) is active toward CrHCO production, but is susceptible to rapid in situ reduction and attendant crotonaldehyde decarbonylation. PdO/Pd(111) can sustain steady-state CrHCO formation under a CrOH/O_2 feedstream.

mixtures at pressures up to 140 mTorr and temperatures up to 150 °C, favoring extensive alcohol decomposition. A Pd_5O_4/Pd(111) surface is active toward crotyl alcohol selox at mild temperatures under flowing CrOH/O_2, but is susceptible to in situ reduction back to the metal, with concomitant decomposition and surface coking. Thicker three-dimensional PdO/Pd(111) films are more resistant to on-stream reduction and able to sustain continuous crotonaldehyde production at 150 °C. The interplay between alcohol and oxygen partial pressures and reaction temperature suggests operation of a Mars–van Krevelen selox mechanism, in which CrOH adsorbed over surface palladium oxides abstracts oxygen to drive CrCHO and coincident water formation, thereby generating metallic sites that must be rapidly reoxidized by gas phase oxygen to prevent their promoting undesired dehydrogenation/hydrogenolysis reactions and consequent self-poisoning. Oxide reducibility thus emerges as a key parameter to optimize high crotonaldehyde yields and prevent on-stream deactivation, necessitating efficient mass transport in liquid phase selox wherein the low solubility of oxygen and slow reoxidation of surface PdO_x anion vacancies may thus become rate-limiting or promoters to act as oxygen buffers and prevent in situ reduction.[44]

■ ASSOCIATED CONTENT

Supporting Information

Table of fitting parameters and additional XPS data. This information is available free of charge via the Internet at http://pubs.acs.org/.

■ AUTHOR INFORMATION

Corresponding Author

*E-mails: Leeaf@cardiff.ac.uk; Wilsonk5@cardiff.ac.uk.

Notes

The authors declare no competing financial interest.

■ ACKNOWLEDGMENTS

We thank the EPSRC for funding (EP/F063423/2), the award of a studentship to J.N.N., and a Leadership Fellowship (EP/G007594/2) to A.F.L. K.W. acknowledges The Royal Society for the award of an Industry Fellowship. The Advanced Light Source is supported by the Director, Office of Science, Office of Basic Energy Sciences, of the U.S. Department of Energy under Contract No. DE-AC02-05CH11231.

■ REFERENCES

(1) Sheldon, R. A.; van Bekkum, H. In *Fine Chemicals through Heterogeneous Catalysis*; Sheldon, R. A.; van Bekkum, H., Eds. Wiley VCH: New York, 2007.
(2) Uozumi, Y.; Yamada, Y. M. A. *Chem. Rec.* **2009**, *9* (1), 51–65.
(3) Vinod, C. P.; Wilson, K.; Lee, A. F. *J. Chem. Technol. Biotechnol.* **2011**, *86* (2), 161–171.
(4) Grunwaldt, J.-D.; Caravati, M.; Baiker, A. *J. Phys. Chem. B* **2006**, *110* (51), 25586–25589.
(5) Keresszegi, C.; Bürgi, T.; Mallat, T.; Baiker, A. *J. Catal.* **2002**, *211* (1), 244–251.
(6) Mallat, T.; Baiker, A. *Chem. Rev.* **2004**, *104* (6), 3037–3058.
(7) Lee, A. F.; Wilson, K. *Green Chem.* **2004**, *6*, 37–42.
(8) Parlett, C. M. A.; Bruce, D. W.; Hondow, N. S.; Lee, A. F.; Wilson, K. *ACS Catal.* **2011**, *1* (6), 636–640.
(9) Hackett, S. E. J.; Brydson, R. M.; Gass, M. H.; Harvey, I.; Newman, A. D.; Wilson, K.; Lee, A. F. *Angew. Chem., Int. Ed.* **2007**, *46* (45), 8593–8596.
(10) Lee, A. F.; Hackett, S. F. J.; Hargreaves, J. S. J.; Wilson, K. *Green Chem.* **2006**, *8* (6), 549–555.
(11) Lee, A. F.; Hackett, S. F. J.; Hutchings, G. J.; Lizzit, S.; Naughton, J.; Wilson, K. *Catal. Tod.* **2009**, *145* (3–4), 251–257.
(12) Naughton, J.; Lee, A. F.; Thompson, S.; Vinod, C. P.; Wilson, K. *Phys. Chem. Chem. Phys.* **2010**, *12* (11), 2670–2678.
(13) Naughton, J.; Pratt, A.; Woffinden, C. W.; Eames, C.; Tear, S. P.; Thompson, S. M.; Lee, A. F.; Wilson, K. *J. Phys. Chem. C* **2011**, *115* (51), 25290–25297.
(14) Lee, A. F.; Chang, Z.; Ellis, P.; Hackett, S. F. J.; Wilson, K. *J. Phys. Chem. C* **2007**, *111* (51), 18844–18847.
(15) Lee, A. F.; Ellis, C. V.; Wilson, K.; Hondow, N. S. *Catal. Tod.* **2010**, *157* (1–4), 243–249.
(16) Siegbahn, H.; Svensson, S.; Lundholm, M. *J. Electron Spectrosc. Relat. Phenom.* **1981**, *24* (2), 205–213.
(17) Siegbahn, H.; Siegbahn, K. *J. Electron Spectrosc. Relat. Phenom.* **1973**, *2* (3), 319–325.
(18) Bluhm, H.; Andersson, K.; Araki, T.; Benzerara, K.; Brown, G. E.; Dynes, J. J.; Ghosal, S.; Gilles, M. K.; Hansen, H. C.; Hemminger, J. C.; Hitchcock, A. P.; Ketteler, G.; Kilcoyne, A. L. D.; Kneedler, E.; Lawrence, J. R.; Leppard, G. G.; Majzlam, J.; Mun, B. S.; Myneni, S. C. B.; Nilsson, A.; Ogasawara, H.; Ogletree, D. F.; Pecher, K.; Salmeron,

M.; Shuh, D. K.; Tonner, B.; Tyliszczak, T.; Warwick, T.; Yoon, T. H. *J. Electron Spectrosc. Relat. Phenom.* **2006**, *150* (2−3), 86−104.
(19) Ogletree, D. F.; Bluhm, H.; Hebenstreit, E. D.; Salmeron, M. *Nucl. Instrum. Methods Phys. Res A* **2009**, *601* (1- 2), 151−160.
(20) Ogletree, D. F.; Bluhm, H.; Lebedev, G.; Fadley, C. S.; Hussain, Z.; Salmeron, M. *Rev. Sci. Instrum.* **2002**, *73* (11), 3872−3877.
(21) Salmeron, M.; Schlogl, R. *Surf. Sci. Rep.* **2008**, *63* (4), 169−199.
(22) Tao, F.; Dag, S.; Wang, L. W.; Liu, Z.; Butcher, D. R.; Bluhm, H.; Salmeron, M.; Somorjai, G. A. *Science* **2010**, *327* (5967), 850−853.
(23) Tao, F.; Salmeron, M. *Science* **2011**, *331* (6014), 171−174.
(24) Grass, M. E.; Karlsson, P. G.; Aksoy, F.; Lundqvist, M.; Wannberg, B.; Mun, B. S.; Hussain, Z.; Liu, Z. *Rev. Sci. Instrum.* **2010**, *81* (5), 053106.
(25) Tao, F.; Grass, M. E.; Zhang, Y. W.; Butcher, D. R.; Renzas, J. R.; Liu, Z.; Chung, J. Y.; Mun, B. S.; Salmeron, M.; Somorjai, G. A. *Science* **2008**, *322* (5903), 932−934.
(26) Knop-Gericke, A.; Kleimenov, E.; Havecker, M.; Blume, R.; Teschner, D.; Zafeiratos, S.; Schlogl, R.; Bukhtiyarov, V. I.; Kaichev, V. V.; Prosvirin, I. P.; Nizovskii, A. I.; Bluhm, H.; Barinov, A.; Dudin, P.; Kiskinova, M. X-Ray Photoelectron Spectroscopy for Investigation of Heterogeneous Catalytic Processes. In *Advances in Catalysis*; Gates, B. C., Knozinger, H., Eds.; Elsevier Academic Press Inc: San Diego, 2009; Vol. *52*, pp 213−272.
(27) Bluhm, H.; Havecker, M.; Knop-Gericke, A.; Kleimenov, E.; Schlogl, R.; Teschner, D.; Bukhtiyarov, V. I.; Ogletree, D. F.; Salmeron, M. *J. Phys. Chem. B* **2004**, *108* (38), 14340−14347.
(28) Lee, A. F.; Prabhakaran, V.; Wilson, K. *Chem. Commun.* **2010**, *46* (22), 3827−3842.
(29) Gabasch, H.; Kleimenov, E.; Teschner, D.; Zafeiratos, S.; Havecker, M.; Knop-Gericke, A.; Schlogl, R.; Zemlyanov, D.; Aszalos-Kiss, B.; Hayek, K.; Klotzer, B. *J. Catal.* **2006**, *242* (2), 340−348.
(30) Gabasch, H.; Unterberger, W.; Hayek, K.; Klotzer, B.; Kleimenov, E.; Teschner, D.; Zafeiratos, S.; Havecker, M.; Knop-Gericke, A.; Schlogl, R.; Han, J. Y.; Ribeiro, F. H.; Aszalos-Kiss, B.; Curtin, T.; Zemlyanov, D. *Surf. Sci.* **2006**, *600* (15), 2980−2989.
(31) Ketteler, G.; Ogletree, D. F.; Bluhm, H.; Liu, H.; Hebenstreit, E. L. D.; Salmeron, M. *J. Am. Chem. Soc.* **2005**, *127* (51), 18269−18273.
(32) Zemlyanov, D.; Aszalos-Kiss, B.; Kleimenov, E.; Teschner, D.; Zafeiratos, S.; Havecker, M.; Knop-Gericke, A.; Schlogl, R.; Gabasch, H.; Unterberger, W.; Hayek, K.; Koltzer, B. *Surf. Sci.* **2006**, *600* (5), 983−994.
(33) Lorenz, M. P. A.; Fuhrmann, T.; Streber, R.; Bayer, A.; Bebensee, F.; Gotterbarm, K.; Kinne, M.; Trankenschuh, B.; Zhu, J. F.; Papp, C.; Denecke, R.; Steinruck, H. P., *J. Chem. Phys.* **2010**, *133* (1), 014706.
(34) Rajumon, M. K.; Roberts, R. S.; Wang, F.; Wells, P. B. *J. Chem. Soc. Faraday Trans.* **1998**, *94* (24), 3699−3703.
(35) Lee, A. F.; Gawthrope, D. E.; Hart, N. J.; Wilson, K. *Surf. Sci.* **2004**, *548*, 200−208.
(36) Lee, A. F.; Wilson, K.; Goldoni, A.; Larciprete, R.; Lizzit, S. *Catal. Lett.* **2002**, *78* (1−4), 379−382.
(37) Lee, A. F.; Ellis, C. V.; Naughton, J. N.; Newton, M. A.; Parlett, C. M. A.; Wilson, K. *J. Am. Chem. Soc.* **2011**, *133* (15), 5724−5727.
(38) Parlett, C. M. A.; Bruce, D. W.; Hondow, N. S.; Newton, M. A.; Lee, A. F.; Wilson, K.; *ChemCatChem* **2012**, DOI: 10.1002/cctc.201200301.
(39) Andersen, J. N.; Hennig, D.; Lundgren, E.; Methfessel, M.; Nyholm, R.; Scheffler, M. *Phys. Rev. B* **1994**, *50* (23), 17525−17533.
(40) Han, J.; Zemlyanov, D. Y.; Ribeiro, F. H. *Surf. Sci.* **2006**, *600* (13), 2730−2744.
(41) Mars, P.; van Krevelen, D. W. *Chem. Eng. Sci.* **1954**, *3*, 41−59.
(42) Vannice, M. A. *Catal. Today* **2007**, *123*, 18−22.
(43) Powell, C. J.; Jablonski, A. *NIST Electron Inelastic-Mean-Free-Path Database. Version 1.2*; National Institute of Standards and Technology: Gaithersburg, MD., 2010.
(44) Lee, A. F.; Gee, J. J.; Theyers, H. J. *Green Chem.* **2000**, *2* (6), 279−282.